Statistical Mechanics of Dense Ionized Matter. I. Equilibrium Properties of the Classical One-Component Plasma

Jean Pierre Hansen
*Laboratoire de Physique Théorique et Hautes Energies, Orsay, France**
(Received 13 April 1973)

The equilibrium properties of a classical one-component plasma, in a uniform background of opposite charge, are computed for systems of various sizes by the Monte Carlo method of Metropolis *et al.* Following the work of Brush, Sahlin, and Teller, the periodicity of the system is accounted for by replacing the long-range Coulomb potential by an effective Ewald sum. Thermodynamic properties are computed over the whole density range of the fluid phase of the system, and their N dependence is carefully investigated. A semiempirical equation of state is proposed from which all thermodynamic properties can be easily derived. Quantum corrections to these properties are calculated to first order in the Wigner expansion. Radial distribution functions, direct-correlation functions, and structure factors at various densities are tabulated. It is shown that at all densities, the direct-correlation function tends rapidly towards its Debye-Hückel form, in contrast to the radial distribution function. The behavior of the structure factor at small wave vectors is also shown to be in good agreement with the Debye-Hückel predictions at all densities.

I. INTRODUCTION

This paper is the first of a series devoted to the study of dense systems of charged particles of one species embedded in a uniform background of opposite charge which ensures over-all electrical neutrality. Most of the calculations presented in this series have been done in the framework of classical statistical mechanics, and the system under consideration is often referred to as a "classical one-component plasma" (ocp). Moreover, many of the results presented in this series have been obtained by the powerful techniques of computer "experiments" which have proved very successful in the study of classical liquids.

The interest of this work appears to be twofold. (a) From the point of view of statistical mechanics and the fluid-solid phase transition, the study of systems of particles interacting through the Coulomb potential completes the recent systematic computer investigations concerned with many-body systems interacting through inverse-power-law potentials:

$$u(r;n)=\epsilon(\sigma/r)^n\,, \tag{1}$$

where r is the interparticle distance.

The case $n=\infty$ corresponds to hard-sphere systems which have received considerable attention since the pioneer work of Alder and Wainwright.[1]

The case $n=12$ is important because of its obvious relation to the familiar Lennard-Jones 12-6 potential, and has also been thoroughly investigated.[2,3]

The cases $n=9, 6$, and 4 have been recently studied by Hoover *et al.*[4]

It thus seemed important to extend these investigations to the case $n=1$, especially since the long-range nature of the Coulomb potential introduces additional interesting features and complications. (b) The ocp is of great astrophysical importance, since it provides an excellent model for describing many features of superdense, completely ionized matter typical of white dwarfs, the outer layers of neutron stars, and possibly the interiors of the heavy planets. The relevance of the model in astrophysics has been pointed out many times; for the case of white-dwarf interiors we refer the reader to the review paper by Van Horn.[5] We only briefly recall that under typical "hot" white-dwarf conditions (temperature $T\simeq 10^8$ °K, density $d\simeq 10^6$ g/cm^3, with predominantly He nuclei) the ratio of the thermal de Broglie wavelength Λ over the ion-sphere radius $a=(\frac{4}{3}\pi\rho)^{-1/3}$ (where ρ is the number density) is

$$\frac{\Lambda}{a}=\left(\frac{2\pi\hbar^2}{MkT}\right)^{1/2}\left(\frac{4\pi\rho}{3}\right)^{1/3}\simeq 0.07\,,$$

whereas the ratio of the temperature over the Fermi temperature of the electrons is

$$\frac{T}{T_f}=\frac{T}{(\hbar^2/2m)(3\pi^2)^{2/3}\,\rho^{2/3}}\simeq 0.05\,.$$

The order of magnitude of the first ratio ensures that quantum effects are small for the nuclei, which can thus be treated essentially by classical statistical mechanics, whereas the second ratio ensures that the electrons are highly degenerate and can therefore be considered as forming an inert uniform background in which the nuclei move. Note that for heavier nuclei the previous ratios would be even smaller.

Thus the ocp model appears to be a reasonable first approximation for the study of superdense ionized matter. Complications due to quantum effects and dielectric screening of the electrons will be examined in subsequent papers.

In fact, Brush, Sahlin, and Teller (BST) have already made an extensive Monte Carlo study of the classical ocp.[6] The great merit of their work was to propose an ingenious treatment of the long-range tail of the potential, taking into account *all* of the periodic images of the particles contained in the initial cell, resulting in the so-called Ewald sum. Their effective potential will be discussed and rederived in a slightly different manner in Sec. II. They were also able to indicate the existence of a liquid-solid phase transition at high density (or low temperature). However, their high-density calculations were insufficient to locate the transition with any degree of confidence. They reported no computations in the stable-solid region, and even at lower densities their Monte Carlo runs lacked sufficient statistics, and probably also sufficient precision in the approximate treatment of the Ewald sums, to yield equilibrium properties of reasonable accuracy. Moreover, they arrived at no definite conclusion concerning the N dependence of their results.

In this paper, we present new Monte Carlo results for the fluid phase of the ocp model which overcome some of the deficiencies of the BST calculations. In particular, the computations are extended to higher densities with the purpose of locating the fluid-solid transition with good accuracy. The following paper[7] is concerned with similar data in the solid phase of the model. Other papers of this series will be devoted to nonequilibrium (or time-dependent) properties of the same model, obtained from molecular-dynamics simulations, as well as to modifications of the results when dielectric screening of the electron background is taken into account. Some of the results presented in this and in the following paper have been briefly reported elsewhere.[8]

This paper is organized as follows. In Sec. II the treatment of the long-range tail for any $1/r^n$ potential is expounded, in the spirit of the BST work. Section III is devoted to the computation of the equilibrium thermodynamic properties of the fluid phase of the ocp. Numerical results from the Monte Carlo simulations are presented and discussed. The N dependence of these data is discussed in Sec. IV. A semiempirical equation of state is derived in Sec. V, and various other equilibrium properties, including the Helmholtz free energy, are derived from it. Quantum corrections to the equation of state are examined in Sec. VI. Section VII is devoted to the presentation and analysis of the Monte Carlo results for radial distribution functions, direct-correlation functions, and structure factors at various densities. Some concluding remarks and indications about future work in this direction are contained in Sec. VIII.

II. TREATMENT OF LONG-RANGE INTERACTIONS

Consider a system of N identical particles interacting through an inverse-power potential $u(r;n)$, defined by (1), and contained in a cubic box of side-length L. As is well known, the excess thermodynamic properties of systems of particles interacting through homogeneous potentials (1) do not depend on temperature and density separately, but only on the dimensionless variable

$$\eta = \left(\frac{4\pi\rho\sigma^3}{3}\right)^{n/3} \frac{\epsilon}{kT} = \left(\frac{\sigma}{a}\right)^n \frac{\epsilon}{kT} ,$$

where a is the "ion-sphere radius." If the distances are expressed in units of a, the potential function divided by kT becomes

$$u(r;n)/kT = \eta/r^n .$$

Note that in the case of the Coulomb potential ($n=1$), $\sigma\cdot\epsilon = (Ze)^2$, where Z is the atomic number of the ion and e the electronic charge; our variable η is then identical with the Γ of BST, and we shall use the label Γ, rather than η, when we specifically consider the Coulomb potential.

In order to minimize surface effects, periodic boundary conditions are assumed, and each particle interacts not only with the $N-1$ other particles contained in the box, but also with *all* periodic images of these particles. Therefore the potential (divided by kT) between a pair of particles in the initial box must be replaced by the sum

$$S(\vec{r},n) = \sum_{\vec{\lambda}} \frac{\eta}{|\vec{r}+L\vec{\lambda}|^n} ,$$

where the sum is over all vectors $\vec{\lambda}$ with integer components; $\vec{r}$ and L are both expressed in units of a. If $n<3$, the sum is divergent and one is forced to introduce a uniform background of "charge" $-\epsilon$, in order to cancel the divergence due to distant images:

$$S(\vec{r},n) = \eta\left(\sum_{\vec{\lambda}} \frac{1}{|\vec{r}+L\vec{\lambda}|^n} - \frac{1}{L^3}\int_{V_\infty} \frac{1}{|\vec{r}+\vec{\rho}|^n}\, d^3\rho\right)$$

$$= \eta\int_{V_\infty} \frac{w(\vec{\rho})}{|\vec{r}+\vec{\rho}|^n}\, d^3\rho , \qquad (2)$$

where the "charge" density $w(\vec{\rho})$ is

$$w(\vec{\rho}) = \sum_{\vec{\lambda}} \delta(\vec{\rho}-L\vec{\lambda}) - \frac{1}{L^3} . \qquad (3)$$

This lattice sum can easily be evaluated using the well-known convergence technique introduced by Ewald[9] and generalized by Nijboer and De Wette.[10] Some details are given in Appendix A; the result is

$$S(\vec{r},n)=\frac{\eta}{\Gamma(\frac{1}{2})L^n}\left\{\sum_{\vec{\lambda}}\frac{\Gamma(\frac{1}{2}n)\pi|\vec{r}/L+\vec{\lambda}|^2}{|\vec{r}/L+\vec{\lambda}|^n}-\frac{4\pi^{(n-1)/2}\Gamma(\frac{3}{2})}{3-n}+\pi^{n-3/2}\sum_{\vec{\lambda}}{}'\lambda^{n-3}\Gamma\left(\frac{3-n}{2},\pi\lambda^2\right)e^{2i\pi\vec{\lambda}\cdot(\vec{r}/L)}\right\}. \tag{4}$$

In this formula, $\Gamma(\nu,x)$ is the incomplete Γ function and the primed summation means that the $\vec{\lambda}=(0,0,0)$ term is excluded. It is interesting to note that the same formula is recovered for $n>3$, in the absence of a uniform background.

The Coulomb case corresponds to $n=1$, and one then recovers the "Ewald potential" derived by BST,

$$\Gamma v(\vec{r})=S(\vec{r},1)=\frac{\Gamma}{L}\left(\sum_{\vec{\lambda}}\frac{\operatorname{erfc}(\pi^{1/2}|\vec{r}/L+\vec{\lambda}|)}{|\vec{r}/L+\vec{\lambda}|}-1+\sum_{\vec{\lambda}}{}'\frac{1}{\pi\lambda^2}e^{-\pi\lambda^2}e^{2i\pi\vec{\lambda}\cdot(\vec{r}/L)}\right). \tag{5}$$

Here $\operatorname{erfc}(x)$ denotes the usual error-function complement, and the variable η is replaced by Γ.

As pointed out by BST, the $\vec{\lambda}=(0,0,0)$ term in the first sum is spherically symmetric, and is dominant at small separations; it has a behavior analogous to a screened Coulomb potential. All other terms are anisotropic, due to the finite size of the system and the periodic boundary conditions; they give the dominant contribution to the pair potential for large separations. The sums over $\vec{\lambda}$ are rapidly convergent and inclusion of the five nearest shells of neighbor boxes is amply sufficient to ensure a relative error of less than 1 part in 10^4. However, computing this truncated sum for all pairs at each step of the Monte Carlo chain is still much too time consuming, and for that reason we have approximated the potential (5) by an optimized expansion in Kubic harmonics, which is discussed in Appendix B. The relative error on the anisotropic part of the potential is always less than 1%, and the relative error on the total potential energy of the system in any configuration is always less than 0.1% if four Kubic harmonics are used in the expansion. These precisions are improved by almost an order of magnitude if an additional harmonic is included in the expansion.

Using (5), the total potential energy of the system divided by kT, in a given configuration, reads

$$\frac{V}{kT}=\Gamma\sum_{i<j}v(\vec{r}_{ij})+\frac{V_0}{kT}, \tag{6}$$

where the second term V_0/kT represents the contribution to the total potential energy of the interactions of each particle with its own periodic images. As pointed out by BST, this term is just equal to $\frac{1}{2}N(E_m/kT)$, where E_m is the Madelung energy of a simple cubic crystal with lattice spacing L:

$$\frac{V_0}{kT}=\frac{NE_m}{2kT}=\frac{-1.791\,858\,5N\Gamma}{2L}. \tag{7}$$

III. COMPUTATION OF THERMODYNAMIC PROPERTIES OF FLUID PHASE

The excess part of the canonical partition function for a system of N particles interacting through the potential (5) is a function of Γ only:

$$Q_N(\Gamma)=\int\cdots\int\exp\left\{-\Gamma\sum_{i<j}v(\vec{r}_{ij})\right\}d^3r_1\cdots d^3r_N.$$

The integration over the $\vec{r}_i$, expressed in units of a, is over a volume $\frac{4}{3}\pi N$.

The total partition function is simply

$$Z_N(\Gamma;a)=\left(\frac{a}{\Lambda}\right)^{3N}\frac{Q_N(\Gamma)}{N!},$$

where Λ is the thermal de Broglie wavelength:

$$\Lambda=\left(\frac{\hbar^2}{2\pi MkT}\right)^{1/2}=\left(\frac{\hbar^2\Gamma a}{2\pi M(Ze)^2}\right)^{1/2}.$$

The excess Helmholtz free energy per ion is related to Q_N by

$$\frac{F}{NkT}(\Gamma)=-\ln Q_N(\Gamma).$$

From this the various excess properties per particle of the ocp are derived by the standard thermodynamic and statistical formulas. Their dimensionless expressions depend only on Γ.

The excess internal energy is

$$\frac{U}{NkT}(\Gamma)=\frac{1}{\Gamma}\frac{\partial(F/NkT)}{\partial\Gamma}=\frac{\Gamma}{Q_N(\Gamma)N}\int\cdots\int\exp\left(-\Gamma\sum_{i<j}v(\vec{r}_{ij})\right)\sum_{i<j}v(\vec{r}_{ij})\,d^3r_1\cdots d^3r_N+\frac{V_0}{NkT}$$
$$=\frac{\Gamma}{N}\left\langle\sum_{i<j}v(\vec{r}_{ij})\right\rangle+\frac{V_0}{NkT}, \tag{8}$$

where the brackets symbolize the average over the canonical ensemble and V_0/NkT is given by (7),

The excess part of the equation of state is

$$\frac{PV}{NkT}(\Gamma)=\frac{\Gamma}{3}\frac{\partial(F/NkT)}{\partial\Gamma}=\frac{1}{3}\left(\frac{U}{NkT}\right)$$
$$=\frac{\Gamma}{3}\left\langle\sum_{i<j}\vec{r}_{ij}\cdot\vec{\nabla}_{ij}v(\vec{r}_{ij})\right\rangle+\frac{V_0}{3NkT}. \quad (9)$$

The excess specific heat at constant volume is

$$\frac{c_v}{Nk}=-\Gamma^2\,\partial[(1/\Gamma)(U/NkT)]/\partial\Gamma$$
$$=\frac{\Gamma^2}{N}\left\{\left\langle\left[\sum_{i<j}v(\vec{r}_{ij})\right]^2-\left\langle\sum_{i<j}v(\vec{r}_{ij})\right\rangle^2\right\rangle\right\}. \quad (10)$$

The inverse excess compressibility K can be calculated from the relation

$$(\rho kTK)^{-1}=\frac{1}{9}\left(\Gamma\frac{\partial(U/NkT)}{\partial\Gamma}+3\frac{U}{NkT}\right)$$
$$=-\frac{c_v}{9Nk}+\frac{4U}{3NkT}. \quad (11)$$

The thermal expansion coefficient α is then obtained from

$$\alpha T=\frac{c_v}{3Nk}\rho kTK=\frac{c_v/Nk}{4(U/NkT)-(c_v/3Nk)}. \quad (12)$$

The specific heat at constant pressure, c_p, is related to c_v by

$$\frac{c_p-c_v}{Nk}=\frac{\alpha^2T^2}{\rho kTK}=\frac{1}{3}\frac{(c_v/Nk)^2}{4(U/NkT)-(C_V/3Nk)}. \quad (13)$$

In order to obtain the full thermodynamic quantities, the ideal-gas values must be added, and these depend on volume and temperature separately. The derivatives of the free energy can be computed by the standard Metropolis-Monte Carlo method.[11] It is well known that the method does not yield the excess free energy (or, equivalently, the partition function) directly, but that quantity can be calculated in the fluid phase by integrating the computed internal energy as a function of Γ:

$$\frac{F}{NkT}=\int_0^\Gamma\frac{U}{NkT}\frac{d\Gamma'}{\Gamma'}. \quad (14)$$

We have computed the excess internal energy, specific heat, and other equilibrium properties for systems of 16, 54, 128, and 250 ions, using the Ewald potential discussed in Sec. II, for values of Γ in the range between 1 and 300. The high-Γ results, corresponding to the solid phase, will be discussed in the following paper. The results presented here correspond to $1\leq\Gamma\leq160$. For $\Gamma\leq100$, the initial configuration of each Monte Carlo run was taken to be a regular bcc lattice configuration; the system then melted rather quickly, and after about 10^4–10^5 configurations a typical fluid-type regime was reached. At higher values of Γ ($100<\Gamma\leq160$), the system melted either more slowly or not at all, and in order to save computer time the initial configuration for the corresponding runs was always taken to be the final configuration of a previous run, corresponding to a lower value of Γ.

For each run between 3×10^5 and 2×10^6 configurations were generated, depending on the value of Γ. To achieve a given precision, more configurations were needed for larger values of Γ, as expected. At least the first 10^5 configurations were rejected before averages of the various thermodynamic properties were taken, in order to allow the system to reach "equilibrium." It should be noted that our statistics are considerably better than those of BST, who generated only about 10^5 configurations in each run. This is insufficient to obtain a reasonable accuracy on the computed averages, especially at high values of Γ.

TABLE I. Monte Carlo results for the 128-particle system as a function of Γ. U/NkT is the excess internal energy per particle divided by kT, $\Delta U/NkT$ is the "thermal" fraction of the excess internal energy, and $(\Delta U/NkT)_{BST}$ is the corresponding BST result for 108 particles (Ref. 6). The results of these first three columns have been corrected for center-of-mass motion [formula (16)], c_v/Nk is the excess specific heat at constant volume per ion, c_v^{BST}/Nk is the corresponding BST result. F/NkT is the *total* free energy per particle (excess + ideal-gas contribution), divided by kT, for kT = 1 Ry [see formula (23)]. g_{max} is the amplitude of the first peak of the rdf, which gives a measure of the short-range order in the fluid. For Γ=2, 3, and 4 the only available BST data are for a 32-particle system.

Γ	$\frac{U}{NkT}$	$\frac{\Delta U}{NkT}$	$\left(\frac{\Delta U}{NkT}\right)_{BST}$	$\frac{c_v}{Nk}$	$\frac{c_v^{BST}}{Nk}$	$\frac{F}{NkT}$	g_{max}
1	−0.580	0.316	0.319	0.11	0.13	−1.160	
2	−1.318	0.473	0.464	0.22	0.21	0.289	
3	−2.111	0.577	0.570	0.28	0.30	0.817	1.010
4	−2.926	0.658	0.648	0.35	0.34	0.960	1.024
10	−7.996	0.971	0.950	0.55	0.59	−0.921	1.135
15	−12.313	1.126	1.09	0.75	0.70	−3.754	1.23
20	−16.667	1.252	1.195	0.80	0.82	−7.024	1.31
30	−25.429	1.450	1.380	1.0	0.97	−14.216	1.44
40	−34.232	1.606	1.478	1.06	0.95	−21.874	1.56
50	−43.094	1.703	1.590	1.16	1.10	−29.796	1.67
60	−51.936	1.821		1.30		−37.888	1.76
70	−60.807	1.909		1.40		−46.099	1.85
80	−69.690	1.986		1.25		−54.399	1.92
90	−78.569	2.066	1.833	1.6		−62.768	1.99
100	−87.480	2.116	1.792	1.5	1.39	−71.192	2.06
110	−96.360	2.195		1.5		−79.660	2.11
120	−105.284	2.230		1.8		−88.165	2.19
125	−109.732	2.262		1.6		−92.430	2.22
130	−114.182	2.292		1.5		−96.702	2.24
140	−123.095	2.34		1.8		−105.267	2.31
155	−136.44	2.43		1.9		−118.156	2.36
160	−140.89	2.46		1.9		−122.463	2.39

The results obtained for the internal energy and specific heat with the 128-particle system are given in Table I and compared to the data of BST obtained with a 108-particle system, when they exist. Because the center of mass of the system is not fixed in the Monte Carlo calculations, the fraction of the internal energy due to the thermal motion of the particles, i.e., the difference between the excess internal energy and its purely static value (the value of the internal energy for a perfect bcc lattice) at the same value of Γ, given by

$$U_0/NkT = -0.895\,929\Gamma, \tag{15}$$

must be multiplied by the factor $N/(N-1)$,[3]

$$\frac{U}{NkT} = \frac{U_0}{NkT} + \left(\frac{U^{MC}}{NkT} - \frac{U_0}{NkT}\right)\frac{N}{N-1}. \tag{16}$$

U^{MC}/NkT stands for the Monte Carlo average of the excess internal energy.

The values of U/NkT listed in Table I have been corrected in this way; we have made the same correction on the BST data.

Table I clearly shows that the purely static energy U_0/NkT accounts for over 95% of the internal energy at all values of Γ, except the lowest. Thus the dominant contribution to the internal energy is, according to formula (15), linear in Γ.

The low-Γ limit will be briefly discussed at the end of this section.

Table I lists the thermal fraction of the internal energy,

$$\frac{\Delta U}{NkT} = \frac{U - U_0}{NkT}. \tag{17}$$

Although this fraction represents only a small part of the total internal energy, it must be calculated with a high accuracy (of the order of 1%) if the transition between the fluid and the solid phases is to be determined accurately, as will become clear in the following paper.

The estimated error in our energy values, a combination of statistical uncertainties in the Monte Carlo runs and a systematic error due to out approximate treatment of the anisotropic part of the Ewald potential, is of the order of a few parts in 10^4; this precision is sufficient to ensure an error of at most 2% on the thermal fraction of the internal energy. As is immediately clear from the data of Table I, the difference between $\Delta U/NkT$ values obtained in the present calculations and those of BST is considerably larger than our estimated error, especially at large values of Γ. The BST values are systematically lower than ours, by as much as 20%. The discussion in Sec. IV clearly shows that this cannot be due to the small difference in N (128 particles versus 108). We believe that the BST values are in error for two reasons: First, the number of configurations over which they average (about 10^5) is too small to yield reliable results for values $\Gamma \gtrsim 10$; secondly, their approximate treatment (Taylor-series expansion) of the anisotropic part of the Ewald potential probably gives rise to large systematic errors.

Regarding the specific heat, the Monte Carlo results, obtained by averaging the fluctuation of the excess internal energy, have statistical uncertainties of the order of 10% for large Γ; our values are in reasonable agreement with the BST data. The equation of state can be derived directly from the internal energy by formula (9). As already noted by BST the ionic pressure (after addition of the ideal-gas term) becomes negative for $\Gamma \gtrsim 4$. However, the total pressure, obtained by adding the contribution of the uniform background, is always positive, as can be easily checked by adding, e.g., the pressure of a degenerate electron gas under density-temperature conditions appropriate for dense stellar interiors. This is only a special case of the well-known general result of Dyson and Lenard[12] that Coulomb systems without any restriction on particle statistics are unstable and that the exclusion principle (Fermi statistics) is essential for stability.

Before analyzing the N dependence of our Monte Carlo results and deriving a semiempirical equation of state, we briefly discuss the behavior of the internal energy in the limit $\Gamma \to 0$. As is well known, the Debye-Hückel (DH) formula gives the leading contribution to the internal energy for very small values of Γ,

$$U^{DH}/NkT = -\tfrac{1}{2}\sqrt{3}\,\Gamma^{3/2}. \tag{18}$$

The next-higher-order terms were calculated by Abe,[13]

TABLE II. Excess internal energy per ion (divided by kT) in low-Γ range as predicted by the linearized DH theory, the Abe nodal expansion [formula (19)], the calculations of Carley (Ref. 14), based on the theory of Broyles, Sahlin, and Carley (Ref. 15) (BSC), and by our Monte Carlo computations.

Γ	$\left(\frac{U}{NkT}\right)_{DH}$	$\left(\frac{U}{NkT}\right)_{Abe}$	$\left(\frac{U}{NkT}\right)_{BSC}$	Monte Carlo
0.01	−0.000 866 0	−0.000 865 6		
0.05	−0.009 68	−0.009 38	−0.0094	
0.1	−0.028 86	−0.002 737	−0.0258	
0.2	−0.077 35	−0.071 68	−0.0688	
$\frac{1}{3}$	−0.1666	−0.1617	−0.144	
1	−0.866	−1.967	−0.577	−0.580
2	−2.449		−1.321	−1.318

$$U^{\mathrm{Abe}}/NkT = -\tfrac{1}{2}\sqrt{3}\,\Gamma^{3/2} - \Gamma^3(\tfrac{9}{8}\ln 3 + \tfrac{3}{2}\gamma - 1) - \tfrac{9}{8}\Gamma^3 \ln\Gamma + O(\Gamma^{9/2}), \quad (19)$$

where γ is Euler's constant.

Carley has calculated the internal energy by using various integral equations for the pair distribution function.[14] His results, obtained with a technique developed by Broyles, Sahlin, and Carley[15] for treating the long-range part of the potential, appear to be the most reliable. The predictions from these various theories are compared with each other in the range $0.01 \leq \Gamma \leq \frac{1}{3}$ in Table II, and with the Monte Carlo results for $\Gamma = 1$ and 2. It is clear from inspection of the table that the DH law is accurate up to $\Gamma \simeq 0.01$. The Abe formula gives good results up to $\Gamma \simeq 0.05$, whereas the results of Broyles, Sahlin, and Carley are still in good agreement with our Monte Carlo data at $\Gamma = 2$. We are presently investigating up to what value of Γ the method of Broyles, Sahlin, and Carley, or a related method due to Lado,[16] predicts reliable energy values.

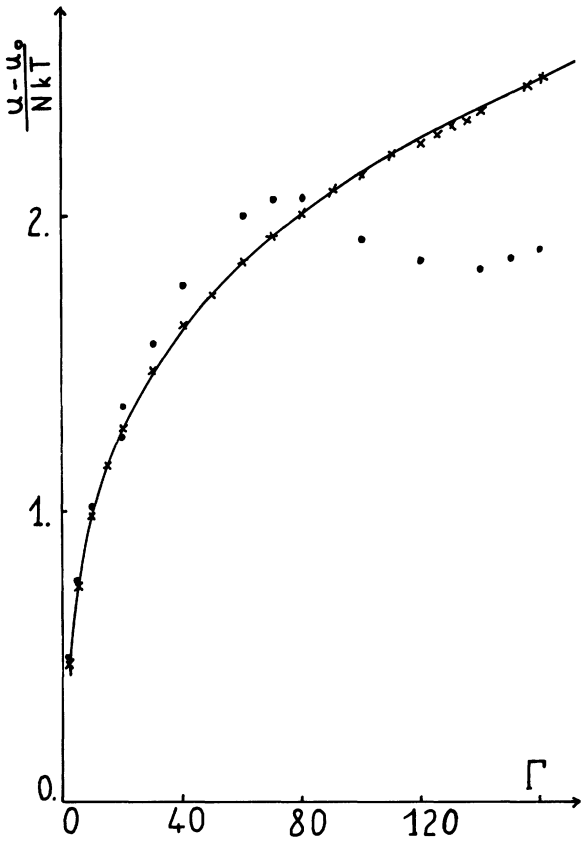

FIG. 1. Thermal fraction of the excess internal energy, $(U - U_0)/NkT$, as a function of Γ; the crosses are the Monte Carlo results for $N = 128$; the dots are the results for $N = 16$.

Finally, it is also clear from the table that the internal-energy values are everywhere bounded from below by their DH values, as has been demonstrated by Mermin.[17] It should also be pointed out that for $\Gamma \gtrsim 1$ the Abe formula predicts energies which are even *lower* than the DH energies. This illustrates the difficulty of calculating convergent correction terms beyond the DH approximation.

IV. N DEPENDENCE OF MONTE CARLO RESULTS

In Sec. III, we have presented the Monte Carlo results for the equilibrium energy pressure and specific heat of a 128-ion system, for values of Γ between 1 and 160. However, for a long-range potential like the Coulomb potential the dependence of the computed thermodynamic properties on the size of the simulated system appears to be a crucial question. For that reason, we have investigated the properties of systems of 16, 54, and 250 ions at various values of Γ, and compared the results obtained for these systems with the data for the 128-particle system.

In Fig. 1 the results for the thermal part of the excess energy (17) are shown as a function of Γ for $N = 16$ and $N = 128$. It is seen that for $\Gamma \lesssim 20$ the difference between the thermal energies remains within the statistical errors. At larger values of Γ there are large deviations, the energy curve of the 16-particle system exhibiting a loop-like behavior in marked contrast with the monotonic increase of the 128-particle thermal-energy curve.

In Table III, we list the Monte Carlo results for $N = 16$, 54, 128, and 250 at three values of Γ: 70, 100, and 140. This last value is close to the fluid-solid transition, as will be shown in the following paper. The energy values are equal within statistical errors for $N = 54$, 128, and 250, at $\Gamma = 70$ and 100; only the results for $N = 16$ differ from the energies obtained for $N = 54$, 128, and 250, by considerably more than the combined statistical errors. We conclude that for $\Gamma \lesssim 100$ our numerical energy values should lie close to their thermodynamic limit for $N \gtrsim 50$. At $\Gamma = 140$ the situation is slightly different, because the energy obtained for $N = 54$ now also differs significantly from the results for $N = 128$ and 250. Thus it appears, not surprisingly, that as one approaches the fluid-solid transition region larger systems are required to yield results close to their thermodynamic limit. Our data seem to indicate, however, that even for Coulomb systems, a system size of a few hundred particles is sufficient to predict energy values close to their thermodynamic limit

TABLE III. Comparison of Monte Carlo results for systems of $N=16$, 54, 128, and 250 ions. $\Delta U/NkT$ is the excess "thermal" energy per particle, divided by kT. c_v/Nk is the excess specific heat per particle at constant volume; g_{max} is the amplitude of the first peak of the rdf.

	$\Gamma=70$				$\Gamma=100$				$\Gamma=140$			
N	16	54	128	250	16	54	128	250	16	54	128	250
$\frac{\Delta U}{NkT}$	2.041	1.944	1.909	1.928	1.90	2.153	2.116	2.148	1.80	2.16	2.34	2.37
c_v/Nk	1.84	1.28	1.43	1.37	2.4	1.42	1.5	1.55	1.4	2.3	1.8	2.15
g_{max}	1.85	1.862	1.848	1.844	2.3	2.10	2.07	2.06	2.82	2.45	2.31	2.32

for all values of Γ, provided the averages are taken over a sufficiently large number of configurations. This apparent paradox is due to the well-known screening effect which strongly reduces the long range of the Coulomb forces. We are now in a position to write down a semiempirical equation of state for the one-component plasma, valid in the range $0<\Gamma\lesssim 160$.

V. EQUATION OF STATE OF CLASSICAL ONE-COMPONENT PLASMA

To calculate the various thermodynamic properties given by formulas (8)–(14), it is useful to have at one's disposal a simple analytic expression giving the excess energy per particle divided by kT (or equivalently, the equation of state), as a function of Γ. We have pointed out in Sec. III that U/NkT behaves like $\Gamma^{3/2}$ in the $\Gamma\to 0$ limit (DH law), and predominantly like Γ in the limit of large Γ. These two features are included in the simple functional form

$$\frac{U}{NkT}=\Gamma^{3/2}\left(\frac{a_1}{(b_1+\Gamma)^{1/2}}+\frac{a_2}{b_2+\Gamma}+\frac{a_3}{(b_3+\Gamma)^{3/2}}+\frac{a_4}{(b_4+\Gamma)^2}\right). \tag{20}$$

a_1 is fixed to yield the correct static term (15) for large values of Γ; a_2, b_2, a_3, b_3, and a_4, b_4 are chosen so as to give a least-squares fit to the Monte Carlo data presented in Table I (128-particle system), which, we have reason to believe is close to the thermodynamic limit values and to the results of Broyles, Sahlin, and Carley[15] for $\Gamma<1$; finally b_1 is chosen so that the coefficient of $\Gamma^{3/2}$ equals $-\frac{1}{2}\sqrt{3}$ in the limit $\Gamma\to 0$ (DH law).

The optimum coefficients thus obtained are

$a_1=-0.895\,929$, $b_1=4.666\,486\,0$;

$a_2=0.113\,406\,56$, $b_2=13.675\,411$;

$a_3=-0.908\,728\,27$, $b_3=1.890\,560\,3$;

$a_4=-0.116\,147\,73$, $b_4=1.027\,755\,4$.

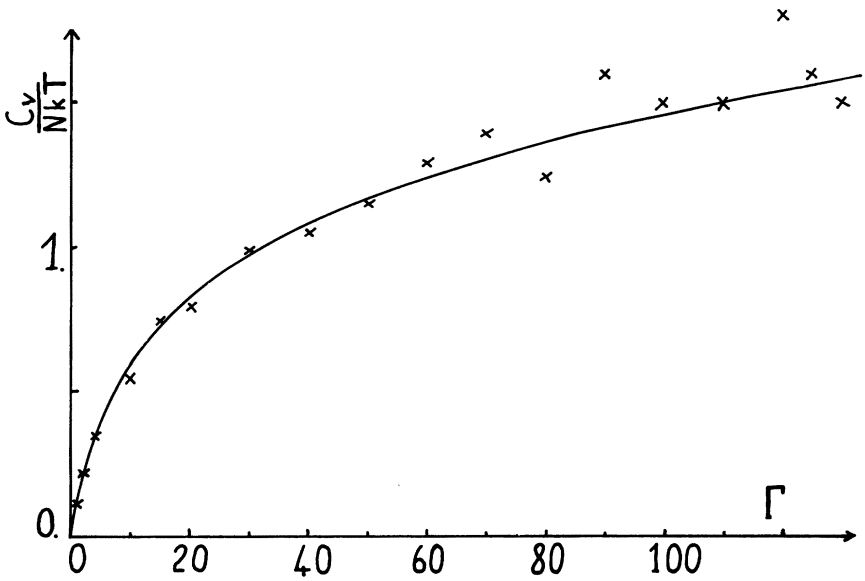

FIG. 2. Excess specific heat at constant volume as a function of Γ. The straight line corresponds to Eq. (21); the dots are the Monte Carlo results.

The data of Table I are then fitted everywhere within their statistical accuracy by formula (20).

By differentiation, the corresponding formula for the specific heat at constant volume reads

$$\frac{c_v}{Nk}=\frac{\Gamma^{5/2}}{2}\left(\frac{a_1}{(b_1+\Gamma)^{3/2}}+\frac{2a_2}{(b_2+\Gamma)^2}+\frac{3a_3}{(b_3+\Gamma)^{5/2}}+\frac{4a_4}{(b_4+\Gamma)}\right)-\frac{\Gamma^{3/2}}{2}\left(\frac{a_1}{(b_1+\Gamma)^{1/2}}+\frac{a_2}{b_2+\Gamma}+\frac{a_3}{(b_3+\Gamma)^{3/2}}+\frac{a_4}{(b_4+\Gamma)^2}\right). \quad (21)$$

In Fig. 2 the c_v/Nk values obtained from Eq. (21) are compared to the values determined directly in the Monte Carlo calculations.

By integration of (20), the excess free energy becomes

$$\frac{F}{NkT}=a_1\mathcal{T}_1(\Gamma)+a_2\mathcal{T}_2(\Gamma)+a_3\mathcal{T}_3(\Gamma)+a_4\mathcal{T}_4(\Gamma),$$

$$\mathcal{T}_1(\Gamma)=\Gamma^{1/2}(b_1+\Gamma)^{1/2}+\tfrac{1}{2}b_1\ln b_1 - b_1\ln[\Gamma^{1/2}+(b_1+\Gamma)^{1/2}],$$

$$\mathcal{T}_2(\Gamma)=2\Gamma^{1/2}-2b_2^{1/2}\arctan\left(\frac{\Gamma^{1/2}}{b_2^{1/2}}\right), \quad (22)$$

$$\mathcal{T}_3(\Gamma)=-\frac{2\Gamma^{1/2}}{(b_3+\Gamma)^{1/2}}-\ln b_3+2\ln[\Gamma^{1/2}+(b_3+\Gamma)^{1/2}],$$

$$\mathcal{T}_4(\Gamma)=-\frac{\Gamma^{1/2}}{b_4+\Gamma}+\frac{1}{b_4^{1/2}}\arctan\frac{\Gamma^{1/2}}{b_4^{1/2}}.$$

The total free energy is obtained by adding the ideal-gas contribution,

$$\frac{F^{(0)}}{NkT}=\ln\left[\rho\left(\frac{2\pi\hbar^2}{MkT}\right)^{3/2}\right]-1$$

$$=-0.7153+3\ln\Gamma+\tfrac{3}{2}\ln(kT)_{\mathrm{Ry}}, \quad (23)$$

where $(kT)_{\mathrm{Ry}}$ means that the energy kT must be expressed in ionic rydberg units. The total free-energy values from (22) and (23) for $(kT)_{\mathrm{Ry}}=1$ are tabulated in the last column of Table I.

VI. QUANTUM CORRECTIONS

So far all our calculations have been made in the framework of classical statistical mechanics; i.e., the ratio Λ/a (de Broglie wavelength divided by the ion sphere radius) was supposed to be 0. This condition is only approximately verified in real dense stellar matter, and during the cooling down of dense stars (e.g., white dwarfs) there will always come a stage where the ratio Λ/a becomes non-negligible. That means that quantum corrections cannot be ignored any longer, and as long as the ratio remains reasonably small, the quantum corrections to the free energy can be calculated by the well-known $\hbar^2$ expansion of Wigner.[18] The leading correction to the free energy in that expansion is

$$\frac{F'}{NkT}=\frac{\hbar^2}{24M(kT)^2}\rho\int g(r)\Delta v(r)\,d^3r,$$

where $g(r)$ is the radial distribution function of the classical system and $\Delta v(r)$ is the Laplacian

TABLE IV. Radial distribution function and direct-correlation function, for $\Gamma=2$, 3, and 4, as a function of interionic distance r in units of $a(\frac{4}{3}\pi)^{1/3}$ (i.e., $\rho^{-1/3}$).

	$\Gamma=2$		$\Gamma=3$		$\Gamma=4$	
r	$g(r)$	$-c(r)$	$g(r)$	$-c(r)$	$g(r)$	$-c(r)$
0.01	0	3.091	0	4.273	0	5.511
0.05	0	3.091	0	4.269	0	5.500
0.09	0	3.089	0	4.259	0	5.476
0.13	0	3.080	0	4.241	0	5.443
0.17	0.006	3.057	0.001	4.213	0	5.403
0.21	0.019	3.018	0.003	4.173	0	5.355
0.25	0.051	2.960	0.014	4.118	0.004	5.293
0.29	0.098	2.883	0.037	4.048	0.009	5.216
0.33	0.157	2.791	0.072	3.959	0.029	5.119
0.37	0.225	2.685	0.119	3.852	0.063	5.002
0.41	0.301	2.569	0.182	3.726	0.112	4.865
0.45	0.380	2.448	0.256	3.583	0.175	4.708
0.49	0.460	2.324	0.339	3.430	0.251	4.531
0.53	0.537	2.202	0.426	3.270	0.338	4.341
0.57	0.608	2.084	0.512	3.109	0.431	4.143
0.61	0.671	1.973	0.593	2.952	0.523	3.943
0.65	0.727	1.870	0.666	2.801	0.612	3.746
0.69	0.774	1.774	0.732	2.658	0.695	3.554
0.73	0.816	1.685	0.790	2.522	0.770	3.370
0.77	0.852	1.602	0.841	2.395	0.834	3.197
0.81	0.883	1.525	0.883	2.277	0.887	3.039
0.85	0.908	1.454	0.917	2.169	0.926	2.896
0.89	0.929	1.389	0.944	2.071	0.956	2.764
0.93	0.945	1.330	0.964	1.981	0.979	2.642
0.97	0.958	1.276	0.978	1.899	0.997	2.529
1.01	0.968	1.226	0.990	1.823	1.009	2.426
1.05	0.977	1.118	0.998	1.753	1.014	2.333
1.09	0.984	1.135	1.004	1.687	1.017	2.247
1.13	0.990	1.094	1.008	1.627	1.019	2.165
1.17	0.993	1.057	1.010	1.572	1.022	2.087
1.21	0.995	1.023	1.009	1.522	1.024	2.014
1.25	0.996	0.992	1.008	1.475	1.022	1.949
1.29	0.997	0.963	1.0065	1.432	1.018	1.892
1.33	0.9975	0.934	1.005	1.390	1.014	1.837
1.37	0.999	0.907	1.0035	1.350	1.019	1.784
1.41	1.000	0.881	1.003	1.313	1.009	1.731
1.45	1.000	0.856	1.003	1.277	1.007	1.682
1.49	1.000	0.834	1.0025	1.242	1.005	1.639
1.53	1.000	0.813	1.0025	1.210	1.002	1.660
1.57	1.000	0.794	1.0020	1.179	0.999	1.561
1.61	1.000	0.774	1.0015	1.151	0.998	1.523
1.65	1.000	0.756	1.0010	1.124	0.998	1.486

of the interatomic potential. In the case of the one-component plasma in a uniform background, the formula becomes

$$\frac{F'}{NkT} = \frac{\hbar^2}{24M(kT)^2}\rho\int[g(r)-1]\Delta\frac{(Ze)^2}{r}\,d^3r$$
$$= \frac{\pi\hbar^2\rho(Ze)^2}{6M(kT)^2} = \frac{\Gamma^3}{16}(kT)_{\mathrm{Ry}}, \qquad (24)$$

where we have used the fact that $g(O)=O$ for all values of Γ. F'/NkT does not depend on Γ alone, but on ρ and T separately (or, alternatively, on Γ and T); this is to be expected, since the introduction of a characteristic length into the problem, in this case the thermal de Broglie wavelength, breaks the scale invariance typical of systems interacting through homogeneous potentials of the form (1).

Formula (24) shows that for a fixed value of Γ quantum corrections *increase* as the temperature increases; this will have important implications in our discussion of the phase transition (following paper).

The corresponding correction to the equation of state is also given by (24), whereas the correction to the excess internal energy per particle is

$$\frac{U'}{NkT} = -2\frac{F'}{NkT} = -\frac{\Gamma^3}{8}(kT)_{\mathrm{Ry}}. \qquad (25)$$

Thus the quantum corrections break the simple relation (9) between internal energy and equation of state.

VII. RADIAL DISTRIBUTION FUNCTIONS AND STRUCTURE FACTORS

Another important quantity which can be calculated relatively easily with good accuracy by Monte Carlo "experiments" is the radial distribution function (rdf) $g(r)$ from which, in principle, the excess internal energy can be calculated:

$$\frac{U}{NkT} = \frac{3\Gamma}{2}\int_0^\infty [g(r)-1]\,r\,dr, \qquad (26)$$

where the r are, as usual, in units of a.

However, formula (26) is in general not very useful because of the long range of the Coulomb potential and the fact that Monte Carlo calculations yield $g(r)$ only for $r \leq \frac{1}{2}L$, where L is the length of the Monte Carlo cell, which is relatively small for systems of a few hundred particles. Only at small values of Γ, where $g(r)$ tends rapidly towards 1, can (26) be used to check the internal-energy value obtained with the Ewald potential. We have found excellent agreement between the two determinations of the energy for $\Gamma \leq 4$; this can be considered to be a good consistency test

TABLE V. Radial distribution functions for $\Gamma=120$, 140, and 160 and the 128-ion system. At $\Gamma=140$ the rdf for the 250-ion system is also tabulated; r is in units of $a(\frac{4}{3}\pi)^{1/3}$ (i.e., $\rho^{-1/3}$).

	$\Gamma=120$	$\Gamma=140$		$\Gamma=160$
r	$N=128$	$N=128$	$N=250$	$N=128$
0.71	0	0	0	0
0.75	0.003	0.001	0.001	0
0.79	0.026	0.013	0.012	0.007
0.83	0.112	0.073	0.070	0.051
0.87	0.343	0.271	0.264	0.219
0.91	0.766	0.677	0.653	0.597
0.95	1.305	1.253	1.238	1.192
0.99	1.820	1.820	1.821	1.820
1.03	2.123	2.190	2.201	2.270
1.07	2.191	2.291	2.321	2.380
1.11	2.060	2.163	2.176	2.252
1.15	1.819	1.901	1.922	1.955
1.19	1.560	1.603	1.613	1.622
1.23	1.319	1.332	1.321	1.335
1.27	1.112	1.100	1.098	1.095
1.31	0.936	0.922	0.918	0.909
1.35	0.815	0.800	0.786	0.772
1.39	0.731	0.711	0.703	0.687
1.43	0.673	0.656	0.638	0.629
1.47	0.648	0.621	0.606	0.602
1.51	0.637	0.618	0.596	0.595
1.55	0.647	0.622	0.616	0.613
1.59	0.672	0.652	0.643	0.645
1.63	0.714	0.694	0.690	0.683
1.67	0.760	0.754	0.746	0.736
1.71	0.829	0.818	0.822	0.803
1.75	0.899	0.891	0.896	0.885
1.79	0.979	0.972	0.987	0.975
1.83	1.046	1.053	1.067	1.056
1.87	1.108	1.124	1.141	1.133
1.91	1.170	1.183	1.199	1.198
1.95	1.213	1.226	1.238	1.246
1.99	1.232	1.246	1.260	1.269
2.03	1.227	1.245	1.256	1.267
2.07	1.205	1.224	1.223	1.238
2.11	1.167	1.189	1.193	1.197
2.15	1.120	1.143	1.138	1.143
2.19	1.071	1.087	1.080	1.088
2.23	1.023	1.032	1.021	1.028
2.27	0.977	0.980	0.969	0.976
2.31	0.941	0.934	0.925	0.934
2.35	0.909	0.892	0.887	0.900
2.39	0.888	0.877	0.855	0.863
2.43	0.876	0.864	0.847	0.850
2.47	0.871	0.860	0.846	0.841
2.51	0.878	0.865	0.854	0.848
2.59			0.893	
2.67			0.973	
2.75			1.034	
2.83			1.079	
2.91			1.095	
2.99			1.077	
3.07			1.049	
3.15			1.010	

for the use of the Ewald potential.

The rdf are interesting for their own sake, because their variation as a function of interionic distance gives indications on the short-range order in the fluid phase. The small-r behavior of $g(r)$ is directly related to the enhancement of nuclear reaction rate in astrophysics, due to the reduction of the Coulomb barrier relative to the two-body case by many-body correlations.[19] Several authors have calculated rdf's for small values of Γ using various integral-equation techniques or cluster expansions.[16,20] In their paper BST made extensive comparisons between some of these results and their Monte Carlo data, and clearly exhibited the limitation of integral equations for the rdf's in the one-component plasma model. The various integral equations yield widely different results already around $\Gamma = 1$ and break down completely for larger values of Γ.

In a recent paper Cooper[21] solved a modified version of the HNC equation valid for the screened Coulomb potential of the Abe-Mayer modal cluster expansion, instead of the bare Coulomb potential, and found results in good agreement with the BST data at $\Gamma = 10$. However, the height of his first peak is slightly less than that of the Monte Carlo result, and this discrepancy between approximate and "exact" rdf at $\Gamma = 10$ is confirmed by our own Monte Carlo results.

Another question which has received considerable attention in recent years is at what value of Γ, $g(r)$ starts to exhibit oscillatory behavior, in contrast to the monotonic behavior [$g(r) \leq 1$ for all r] typical of the nonlinearized DH predictions at low Γ.[20-22] The integral-equation results of Cooper indicate that the onset of short-range order takes place for $2 < \Gamma < 3$. This is confirmed by our Monte Carlo calculations with the 128-particle system, as illustrated by the data of Table IV, which lists our $g(r)$ results for $\Gamma = 2, 3$, and 4.

At higher values of Γ, up to $\Gamma = 100$, our rdf's are in reasonable agreement with the BST data, and for that reason our results are not tabulated here. In Table V we list the rdf's computed for $\Gamma = 120$, 140, and 160; (in that range no data had been previously tabulated by BST). At $\Gamma = 140$ the results for both the 128- and 250-particle systems are listed; the differences are within statistical errors for all values of r (about 1%, except for small r, where they are larger because of poor statistics).

The Fourier transform of the radial distribution function is the structure factor

$$S(k) = 1 + 3\Gamma \int_0^\infty \frac{\sin kr}{kr} [g(r) - 1] r^2 \, dr \,. \tag{27}$$

In the DH limit, $S(k)$ reads

$$S_{\mathrm{DH}}(k) = \frac{k^2}{k^2 + 3\Gamma} \,. \tag{28}$$

The well-known Stillinger-Lovett conditions[23] on the zeroth and second moments of the radial distribution functions of Coulomb systems applied to the one-component plasma imply that the small-k behavior of the exact $S(k)$ is equal to that of the DH solution. More specifically, the zeroth moment (or electroneutrality) condition implies

$$S(0) = O \,. \tag{29}$$

The second-moment condition implies

$$S(k) \simeq k^2/3\Gamma \quad \text{for } k \to 0, \tag{30}$$

where the wave vector is in units of a^{-1}. Again, because $g(r)$ is only calculated for $r \leq L/2$ by the Monte Carlo runs, formula (27) is useless to extract $S(k)$, especially for small k, except for small values of Γ, when $g(r)$ tends rapidly towards 1. $S(k)$ was obtained by the simple Fourier inversion (27) for $\Gamma \leq 4$. For larger values of Γ, $S(k)$ had to be calculated directly from its definition,

$$S(k) = (1/N) \langle \rho_{\vec{k}} \, \rho_{-\vec{k}} \rangle \,, \tag{31}$$

by averaging the product of collective coordinates,

$$\rho_{\vec{k}} = \sum_i e^{i \vec{k} \cdot \vec{r}_i} \,, \tag{32}$$

over several hundred independent configurations generated during the Monte Carlo runs. The $\vec{k}$ vectors in (32) are those of the reciprocal lattice associated with the periodic repetition of the elementary Monte Carlo cell containing N particles. The length of the smallest $\vec{k}$ vector compatible with the size of this cell is thus $2\pi/L$. It is remarkable that for the 250-particle system the small-k results for $S(k)$ are in good agreement with the predictions of formula (28) at Γ values as large as $\Gamma = 100$ and 140, as shown by Table VI. Thus a system of a few hundred ions is already capable of exhibiting essentially collective behavior over distances of roughly 10 ionic radii.

The structure factors obtained for $\Gamma = 4$ and 10 from the 128-particle system, and for $\Gamma = 100$ and 140 from the 250-particle system, are tabulated in Table VI. $S(k)$ has also been computed for the 128-particle system at $\Gamma = 140$, which is close to the fluid-solid transition, and compared to the structure factors at crystallization of hard spheres and various other inverse-power potentials by Hansen and Schiff.[24] The essential conclusion of that work was the great similarity between the main peaks of the various structure factors at crystallization, which are nearly independent of the exact nature of the interatomic repulsion.

$S(k)$ computed for $N=250$ and $\Gamma=140$ is in excellent agreement with the previous computation for $N=128$. Finally, the Fourier transform of the Ornstein-Zernike direct-correlation function, $\tilde{C}(k)$, is obtained immediately from $S(k)$ through the defining relation

$$\tilde{C}(k)=\tfrac{4}{3}\pi\,\frac{S(k)-1}{S(k)}\,, \tag{33}$$

which behaves like $-4\pi\Gamma/k^2$ at small k [see Eq. (30)].

From this, the direct-correlation function (dcf) can be obtained by Fourier inversion:

$$c(r)=\frac{2}{\pi}\int_0^\infty \tilde{C}(k)\frac{\sin kr}{kr}\,k^2\,dk\,. \tag{34}$$

Table IV lists $c(r)$ together with $g(r)$ for $\Gamma=2$, 3, and 4. A remarkable feature of the $c(r)$ extracted from our Monte Carlo data is that they tend rapidly, for increasing r, towards their DH limit,

$$c^{\mathrm{DH}}(r)=-\Gamma/r\,, \tag{35}$$

and this for all values of Γ.

Only the short-range behavior of $c(r)$ differs considerably from the DH limit. The "exact" dcf is negative everywhere and goes to a finite limit as $r\to 0$, contrary to $c^{\mathrm{DH}}(r)$. The situation is illustrated by Fig. 3, where we have drawn $c(r)$ and $c^{\mathrm{DH}}(r)$ for $\Gamma=100$. The two dcf's are seen to differ markedly only for $r\lesssim 1$ (in units of a). This remarkable feature illustrates the spirit of the Orn-

TABLE VI. Structure factors at $\Gamma=4$, 10, 100, and 140 as a function of the wave vector $\vec{k}$, in units of $a^{-1}(\frac{3}{4}\pi)^{1/3}$ (i.e., $\rho^{1/3}$). At $\Gamma=4$ and 10, $S(k)$ was obtained through formula (27) from the Monte Carlo rdf. At $\Gamma=100$ and 140, $S(k)$ was computed directly [formula (31)] with the 250-particle system.

k	$\Gamma=4$	$\Gamma=10$	$\Gamma=100$	$\Gamma=140$
1.0	0.032	0.011	0.0013	0.0009
1.4	0.063	0.024	0.0027	0.0019
1.8	0.106	0.042	0.0047	0.0035
2.2	0.162	0.071	0.0079	0.0059
2.6	0.230	0.110	0.0127	0.0094
3.0	0.304	0.158	0.0188	0.0143
3.4	0.390	0.221	0.0259	0.0225
3.8	0.484	0.299	0.0396	0.033
4.2	0.582	0.400	0.069	0.049
4.6	0.675	0.512	0.108	0.078
5.0	0.764	0.642	0.183	0.140
5.4	0.841	0.784	0.290	0.248
5.8	0.904	0.914	0.650	0.522
6.2	0.954	1.025	1.345	1.035
6.6	0.987	1.094	1.944	2.18
7.0	1.010	1.135	2.130	2.66
7.4	1.021	1.141	1.860	1.92
7.8	1.028	1.122	1.402	1.33
8.2	1.029	1.098	1.011	0.96
8.6	1.028	1.071	0.820	0.81
9.0	1.026	1.045	0.767	0.71
9.4	1.024	1.026	0.748	0.66
9.8	1.020	1.010	0.728	0.655
10.2	1.016	0.999	0.734	0.68
10.6	1.012	0.991	0.783	0.76
11.0	1.009	0.986	0.864	0.84
11.4	1.006	0.983	0.940	0.935
11.8	1.003	0.982	1.000	1.06
12.2	1.002	0.984	1.058	1.13
12.6	1.001	0.987	1.113	1.185
13.0	1.000	0.990	1.149	1.20
13.4	0.999	0.994	1.147	1.17
13.8	0.998	0.996	1.114	1.12
14.2	0.998	0.998	1.062	1.07
14.6	0.998	0.999	1.020	1.00
15.0	0.999	0.999	0.988	0.94
15.4	0.999	1.000	0.963	0.92
15.8	1.000	1.000	0.945	0.90
16.2	1.000	1.001	0.937	0.91
17.0			0.956	
17.8			0.983	
18.6			1.013	
19.4			1.029	
20.2			1.020	
21.0			1.009	

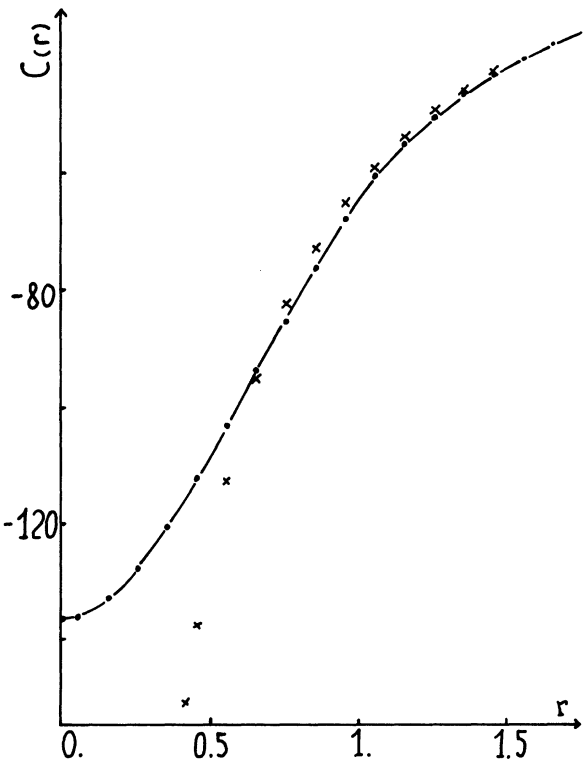

FIG. 3. Direct-correlation function $c(r)$ as a function of interionic distance r (in units of $a(\frac{4}{3}\pi)^{1/3}$). The dots correspond to the Monte Carlo results, the crosses to the linearized DH approximation.

stein-Zernike theory, in which much of the important information on pair correlation is concentrated in the short-range behavior of $c(r)$, which goes to its DH limit much faster than the rdf.

VIII. CONCLUSIONS

This paper on the classical one-component plasma describes work on the fluid phase of that model which, although it partly goes in the same direction as the beautiful work of Brush, Sahlin, and Teller,[6] brings important improvements and several new contributions. At low values of Γ our equation-of-state data and radial distribution functions are in good agreement with the work of Broyles, Sahlin, and Carley,[15] the recent work of Cooper,[21] and the earlier Monte Carlo results of BST. For $\Gamma \gtrsim 10$, where computer "experiments" seem to be the only reliable tool for computing thermodynamic properties of the one-component plasma, our equation-of-state data differ markedly from the BST results, although the rdf's are in good agreement. This apparent contradiction is probably due to the fact that the rdf are rather insensitive to the details of the weakly varying anisotropic part of the Ewald potential. For $\Gamma > 100$ the data presented here are entirely new. The N dependence of the various computed quantities has been carefully checked, and it seems that a system of $N \gtrsim 100$ ions yields results very close to the thermodynamic limit in the whole fluid range.

Our Monte Carlo data for all Γ are summarized in a relatively simple semiempirical equation of state from which all other thermodynamic properties can easily be extracted. The first Wigner quantum correction to that equation of state has also been calculated. Finally, we have computed the structure factor and the direct-correlation function for various Γ. The dcf results are particularly interesting because they exhibit a fast convergence towards the DH limit, even at high Γ, in marked contradiction to the rdf.

The following paper is devoted to the study of the solid phase of the one-component plasma, to the melting transition of that system, as well as to the extension of the phase diagram to the whole ρ-T plane. Time-dependent properties of the model will be examined in a later paper, and the effect of dielectric screening will be considered in the following and further papers of the series.

ACKNOWLEDGMENTS

The author is indebted to B. Jancovici for a careful reading of the manuscript and helpful suggestions, and to B. J. Adler for stimulating discussions.

APPENDIX A: DERIVATION OF THE EWALD FORM OF AN INVERSE-POWER PAIR POTENTIAL

The purpose of this appendix is to show briefly how the effective pair potential (2) for a finite periodic system of particles interacting through an inverse-power potential (1) in a uniform background of opposite "charge" can be expressed as a rapidly converging Ewald sum, by the technique of Nijboer and De Wette.[10] Consider

$$S(\vec{r},n) = \int \frac{w(\vec{\rho})}{|\vec{r}+\vec{\rho}|^n}\, d^3\rho\,, \tag{A1}$$

$$w(\vec{\rho}) = \sum_{\vec{\chi}} \delta(\vec{\rho} - L\vec{\chi}) - \frac{1}{L^3}\,. \tag{A2}$$

The sum over $\vec{\chi}$ goes over all vectors with integer coordinates.

Introduce an auxiliary "convergence" function $\eta(x)$ and rewrite (A1):

$$S(\vec{r},n) = \int \frac{w(\vec{\rho})\eta(|\vec{r}+\vec{\rho}|)}{|\vec{r}+\vec{\rho}|^n}\, d^3\rho + \int \frac{w(\vec{\rho})[1-\eta(|\vec{r}+\vec{\rho}|)]}{|\vec{r}+\vec{\rho}|^n}\, d^3\rho\,. \tag{A3}$$

A convenient choice for η is[10]

$$\eta(|\vec{r}+\vec{\rho}|) = \frac{\Gamma(n/2, \alpha\{[|\vec{r}+\vec{\rho}|^2]/L^2\})}{\Gamma(\frac{1}{2}n)}\,, \tag{A4}$$

where $\Gamma(\frac{1}{2}n, x)$ is the incomplete Γ function defined by

$$\begin{aligned} \Gamma(\tfrac{1}{2}n, x) &= \int_x^\infty e^{-t} t^{n/2-1}\, dt\,, \\ 1-\eta(|\vec{r}+\vec{\rho}|) &= 1 - \frac{\Gamma(\frac{1}{2}n, \alpha\{[|\vec{r}+\vec{\rho}|^2]/L^2\})}{\Gamma(\frac{1}{2}n)} \\ &= \frac{\gamma(\frac{1}{2}n, \alpha\{[|\vec{r}+\vec{\rho}|^2]/L^2\})}{\Gamma(\frac{1}{2}n)}\,, \end{aligned} \tag{A5}$$

where

$$\gamma(\tfrac{1}{2}n, x) = \int_0^x e^{-t} t^{n/2-1}\, dt\,.$$

The parameter α in (A4) and (A5) is arbitrary and must be chosen finally so as to ensure good convergence of the Ewald sum. BST made the choice $\alpha = \pi$ in the case of the Coulomb potential ($n = 1$); this choice is not optimal, but in order to avoid any confusions we shall adopt the same choice in the following.

$S(\vec{r},n)$ now reads

$$S(\vec{r},n) = \frac{1}{\Gamma(\frac{1}{2}n)} \left(\int \frac{w(\vec{\rho})\Gamma(\frac{1}{2}n, \pi[|\vec{r}+\vec{\rho}|^2]/L^2)}{|\vec{r}+\vec{\rho}|^n}\, d^3\rho + \int \frac{w(\vec{\rho})\gamma(\frac{1}{2}n, \pi[|\vec{r}+\vec{\rho}|^2]/L^2)}{|\vec{r}+\vec{\rho}|^n}\, d^3\rho \right). \tag{A6}$$

The first term on the right-hand side is rapidly convergent, because of the presence of the Γ function, and thus presents no problem.

The second term is transformed using Parseval's theorem:

$$I = \int w(\vec{\rho}) f(\vec{\rho})\, d^3\rho = \int \tilde{w}(\vec{k}) \tilde{f}(k)\, d^3k ,$$

where

$$f(\vec{\rho}) = \frac{\gamma(\frac{1}{2}n, \pi|\vec{r}+\vec{\rho}|^2/L^2)}{|\vec{r}+\vec{\rho}|^n} ,$$

$$\tilde{f}(k) = \pi^{n-3/2} k^{n-3} \Gamma[\tfrac{1}{2}(3-n), \pi k^2 L^2] e^{2i\pi \vec{k}\cdot\vec{r}} , \qquad \text{(A7)}$$

$$\tilde{w}(\vec{k}) = \sum_{\vec{\lambda}} e^{2i\pi L \vec{k}\cdot\vec{\lambda}} - \frac{1}{L^3}\delta(\vec{k}) .$$

Owing to the periodicity of the lattice,[10] $\tilde{w}(k)$ can be rewritten

$$\tilde{w}(k) = \frac{1}{L^3}\sum_{\vec{\lambda}} \delta\left(\vec{k} - \frac{\vec{\lambda}}{L}\right) - \frac{1}{\lambda^3}\delta(\vec{k})$$

$$= \frac{1}{L^3}\sum_{\vec{\lambda}}{}' \delta\left(\vec{k} - \frac{\vec{\lambda}}{L}\right). \qquad \text{(A8)}$$

The primed summation means as usual that the term $\vec{\lambda}=0$ is omitted. Hence I reduces to

$$I = \frac{\pi^{n-3/2}}{L^n}\sum_{\vec{\lambda}}{}' \lambda^{n-3}\Gamma[\tfrac{1}{2}(3-n), \pi\lambda^2] e^{2i\pi\vec{\lambda}\cdot\vec{r}/L} , \qquad \text{(A9)}$$

with $\lambda = |\vec{\lambda}|$.

Putting (A2) and (A9) into (A6) and integrating the incomplete Γ function finally yields

$$S(\vec{r}, n) = \frac{1}{\Gamma(\frac{1}{2}n)L^n}\left(\sum_{\vec{\lambda}} \frac{\Gamma(n/2, \pi(|\vec{r}+L\vec{\lambda}|^2/L^2)}{|\vec{r}/L+\vec{\lambda}|^n} - \frac{4\pi^{n-1/2}\Gamma(\frac{3}{2})}{3-n} + \pi^{n-3/2}\sum_{\vec{\lambda}}{}' \lambda^{n-3}\Gamma[\tfrac{1}{2}(3-n), \pi\lambda^2] e^{2i\pi\vec{\lambda}\cdot\vec{r}/L}\right).$$

APPENDIX B: APPROXIMATION OF EWALD POTENTIAL BY KUBIC HARMONIC EXPANSION

The Ewald potential (5) has cubic symmetry by construction. It is made up of an isotropic term

$$v(r) = \frac{\operatorname{erfc}(\pi^{1/2} r/L)}{r} - \frac{1}{L}, \qquad \text{(B1)}$$

which tends towards the bare Coulomb potential as $r \to 0$, and a cubically symmetric term

$$v'(\vec{r}) = \frac{1}{L}\sum_{\vec{\lambda}}{}'\left(\frac{\operatorname{erfc}(\pi^{1/2}|\vec{r}/L+\vec{\lambda}|)}{|\vec{r}/L+\vec{\lambda}|} + \frac{e^{-\pi\lambda^2}}{\pi\lambda^2} e^{2i\pi\vec{\lambda}\cdot\vec{r}/L}\right). \qquad \text{(B2)}$$

The isotropic term can be handled easily in the Monte Carlo program by simply tabulating the $v(r)$ as a function of the interionic distance $r \in [0, \sqrt{3}\frac{1}{2}L/]$.

The nonisotropic term is more difficult to handle. A three-dimensional tabulation with interpolations is feasible, but the computer memory requirements are important, for a given precision, even if one allows for the important reductions due to the cubic symmetry.

An alternative way of proceeding is to expand the potential $v'(r)$ in its natural basis, i.e., the Kubic harmonics introduced by Von der Lage and Bethe.[25] The coefficients of the Kubic harmonics in such an expansion are simple functions of the radial distance r, which can be easily calculated by projecting (B2) on each of these harmonics. Calculating these functions up to the K_8 harmonic shows good convergence of the series inside the sphere inscribed to the basic Monte Carlo cell. The convergence appears, however, to be poor outside that sphere. For that reason we have preferred to approximate (B2) by a function of the form

$$v'(r) = v_0(r) + v_4(r)\left[\frac{x^4+y^4+z^4}{r^4}\right] + v_6(r)\frac{x^2y^2z^2}{r^6} + v_8(r)\left[\frac{x^8+y^8+z^8}{r^8}\right] + \ldots , \qquad \text{(B3)}$$

where $v_0(r)$, $v_4(r)$, $v_6(r)$, $v_8(r)$, ... are chosen to be simple polynomials in r^2, rather than the exact coefficients of the Kubic harmonics. The coefficients of the various powers of the polynomials are adjusted so as to yield a least-squares fit to the pair potential (B2). For that reason we call the form (B3) of the nonisotropic potential an "optimized" expansion in Kubic harmonics. If this expansion is truncated after K_8, a set of optimized functions v_0, v_4, v_6, and v_8 is

$$v_0(r) = a_0 + e^{-\pi r^2}(a_4 r^4 + a_6 r^6 + a_8 r^8 + a_{10} r^{10}),$$

$$v_4(r) = e^{-\pi r^2}(b_4 r^4 + b_6 r^6 + b_8 r^8 + b_{10} r^{10}),$$

$$v_6(r) = e^{-\pi r^2}(c_6 r^6 + c_8 r^8 + c_{10} r^{10} + c_{12} r^{12}),$$

$$v_8(r) = e^{-\pi r^2}(d_8 r^8 + d_{10} r^{10} + d_{12} r^{12}).$$

a_0 has been fixed to give the exact value of $v'(r)$ at the origin.

$a_0 = 0.162\,703$;

$a_4 = -3.090\,150$, $b_4 = 9.801\,067\,1$;

$a_6 = 4.676\,413\,1$, $b_6 = -19.994\,017$;

$a_8 = 97.681\,783$, $b_8 = -237.904\,23$;

$a_{10} = -110.956\,81$, $b_{10} = 312.866\,29$;

$c_6 = -22.645\,201$;

$c_8 = -656.4341$, $d_8 = 357.747\,14$;

$c_{10} = 440.658\,02$, $d_{10} = -570.955\,01$;

$c_{12} = 96.923\,540$, $d_{12} = 133.224\,53$.

The relative error on the nonisotropic part of the potential is small (of the order of 1% or less) for all interionic positron vectors $\vec{r}$. The error is of variable sign for various $\vec{r}$ and, consequently, the error on the total potential energy is considerably smaller, less than 0.1% for all configurations, and also of variable sign.

As averages over many configurations are taken in the Monte Carlo runs, the error on, e.g., the potential energy is expected to be negligible, compared to the statistical uncertainties. This was explicitly checked by making two independent Monte Carlo runs at $\Gamma = 100$, one using the previous approximation of the pair potential, another using a still better approximation of that potential obtained with five Kubic harmonics instead of four. The final results for the various equilibrium properties differed by less than the combined statistical uncertainties.

---

*Laboratoire associé au Centre National de la Recherche Scientifique. Addresse: Bâtiment 211, Université Paris-Sud, 91405 Orsay, France.

[1]B. J. Alder and T. E. Wainwright, J. Chem. Phys. 27, 1208 (1957).
[2]J. P. Hansen, Phys. Rev. A 2, 221 (1970).
[3]W. G. Hoover, M. Ross, K. W. Johnson, D. Henderson, J. A. Barker, and B. C. Brown, J. Chem. Phys. 52, 4931 (1970).
[4]W. G. Hoover, S. G. Gray, and K. W. Johnson, J. Chem. Phys. 55, 1128 (1971).
[5]H. M. Van Horn, in *White Dwarfs*, edited by W. J. Luyten (Springer, Berlin, 1971), p. 96.
[6]S. G. Brush, H. L. Sahlin, and E. Teller, J. Chem. Phys. 45, 2102 (1966).
[7]E. L. Pollock and J. P. Hansen, following paper, Phys. Rev. A 8, 3110 (1973).
[8]J. P. Hansen, Phys. Lett. A 41, 213 (1972).
[9]P. P. Ewald, Ann. Phys. (Leipz.) 64, 253 (1921).
[10]B. R. A. Nijboer and F. W. De Wette, Physica 23, 309 (1957).
[11]N. Metropolis, A. W. Rosenbluth, M. N. Rosenbluth, A. M. Teller, and E. Teller, J. Chem. Phys. 21, 1087 (1953); see also W. W. Wood and F. R. Parker, J. Chem. Phys. 27, 720 (1957).
[12]F. J. Dyson and A. Lenard, J. Math. Phys. 8, 423 (1967); A. Lenard and F. J. Dyson, J. Math. Phys. 9, 698 (1968).
[13]R. Abe, Prog. Theor. Phys. 22, 213 (1959).
[14]D. D. Carley, Phys. Rev. 131, 1406 (1963).
[15]A. A. Broyles, H. L. Sahlin, and D. D. Carley, Phys. Rev. Lett. 10, 319 (1963).
[16]F. Lado, Phys. Rev. 135, A1013 (1964).
[17]N. D. Mermin, Phys. Rev. 171, 272 (1968).
[18]E. Wigner, Phys. Rev. 40, 749 (1932).
[19]E. E. Salpeter and H. M. Van Horn, Astrophys. J. 155, 183 (1969).
[20]D. D. Carley, J. Chem. Phys. 43, 3489 (1966). F. Del Rio and H. E. DeWitt, Phys. Fluids 12, 791 (1969).
[21]M. S. Cooper, Phys. Rev. A 7, 1 (1973).
[22]Ph. Choquard and R. R. Sari, Phys. Lett A 40, 109 (1972).
[23]F. H. Stillinger and R. Lovett, J. Chem. Phys. 49, 1991 (1968).
[24]J. P. Hansen and D. Shiff, Mol. Phys. (to be published).
[25]F. C. Von der Lage and H. A. Bethe, Phys. Rev. 71, 612 (1947).